Stenoparib, an inhibitor of cellular poly (ADP-ribose) polymerases (PARPs), blocks *in vitro* replication of SARS-CoV-2 variants

Katherine E Zarn[1¶], Sierra A Jaramillo[1¶], Anthony R Zapata[1], Nathan E Stone[1], Ashley N Jones[1], Haley E Nunnally[1], Erik W Settles[1,2], Ken Ng[1], Paul S Keim[1,2], Steen Knudsen[3], Patricia M Nuijten[4], Aloys SL Tijsma[4], Christopher T French[1,2,5]*

[1] Pathogen and Microbiome Institute, Northern Arizona University, Flagstaff, Arizona, United States of America

[2] Department of Biological Sciences, Northern Arizona University, Flagstaff, Arizona, United States of America

[3] Allarity Therapeutics Europe, DK-2970 Hørsholm, Denmark

[4] Viroclinics-DDL, Rotterdam, The Netherlands

[5] COVID-19 Testing Service Center (CTSC), Pathogen and Microbiome Institute, Northern Arizona University, Flagstaff, Arizona, United States of America

* Corresponding Author

Email: ctfrench@nau.edu (CTF)

¶ These authors contributed equally to this work.

Abstract

We recently published a preliminary assessment of the activity of a poly (ADP-ribose) polymerase (PARP) inhibitor, stenoparib, also known as 2X-121, which inhibits viral replication by affecting pathways of the host. Here we show that stenoparib effectively inhibits a SARS-CoV-2 *wt* (BavPat1/2020) strain and four additional variant strains; *alpha* (B.1.1.7), *beta* (B.1.351), *delta* (B.1.617.2) and *gamma* (P.1) *in vitro*, with 50% effective concentration (EC_{50}) estimates of 4.1 μM, 8.5 μM, 24.1 μM, 8.2 μM and 13.6 μM, respectively. A separate experiment focusing on a combination of 10 μM stenoparib and 0.5 μM remdesivir, an antiviral drug, resulted in over 80% inhibition of the *alpha* (B.1.1.7) variant, which is substantially greater than the effect achieved with either drug alone, suggesting at least additive effects from combining the different mechanisms of activity of stenoparib and remdesivir.

Introduction

36 As of March 2022, the coronavirus disease (COVID-19) pandemic, caused by SARS-CoV-2, has caused over 446 million infections and over 6 million deaths worldwide [1]. Although
38 protective vaccines are available, the pandemic continues, and both old and new SARS-CoV-2 variants exhibit varying degrees of disease severity and resistance to vaccination. Additional
40 effective therapeutics are urgently needed. Here we describe the antiviral activity of a small molecule, stenoparib, an inhibitor of mammalian poly (ADP-ribose) polymerases (PARPs). We
42 show that stenoparib effectively inhibits replication of SARS-CoV-2 wild-type (*wt*) and variant strains *in vitro*.

44 SARS-CoV-2 has undergone adaptation and mutation since the beginning of the COVID-19 pandemic, resulting in new variants of the virus. Only two antiviral drugs, remdesivir and
46 molnupiravir, or treatment with monoclonal antibodies, have been approved by the United States Food and Drug Administration as COVID-19 therapies under the Emergency Use Authorization
48 [2, 3]. Remdesivir and molnupiravir are nucleoside analogs that affect the activity of the RNA-dependent RNA polymerase (RdRp). After incorporation into viral RNA, remdesivir stalls the
50 RdRp during elongation [4], while molnupiravir results in the incorporation of mutations that can be functionally deleterious [5].

52 We recently published a study on the activity of a poly (ADP-ribose) polymerase (PARP) inhibitor, stenoparib, also known as 2X-121, which inhibits viral replication by affecting
54 pathways of the host [6] as opposed to targeting viral replication. ADP-ribosylation (ADPR) pathways may have either anti- or pro-viral properties, and their importance in host-virus
56 interactions is becoming increasingly recognized [7]. Unlike remdesivir, which inhibits viral replication downstream of entry into the cell, stenoparib inhibits virus entry and post-entry

58 processes [6]. Stenoparib inhibited the SARS-CoV-2 USA-WA1/2020 virus and the HCoV-NL63 human seasonal respiratory coronavirus *in vitro*, exhibiting dose-dependent suppression of
60 virus multiplication and cell-cell spread in cell culture [6]. Stenoparib exhibits a unique dual activity against the PARP1, 2 and PARP5a, 5b (tankyrase 1, 2) enzymes, which are important
62 intermediates in the Wnt/β-catenin immune checkpoint [8, 9]. As a host-targeting therapeutic that does not directly select for resistance in viruses, we hypothesize that stenoparib should be able to
64 inhibit all SARS-CoV-2 variant strains.

66 Materials and Methods

Cell Culture

68 For the ViroSpot reduction assays, the antiviral activity of stenoparib on SARS-CoV-2 was assessed *in vitro* using Vero E6 *Cercopithecus aethiops* kidney cells (cat # CRL-1586, ATCC,
70 Manassas, VA, USA) maintained in Dulbecco's Modified Eagle Medium (DMEM; cat #BE12-733F, Lonza, Basel, Switzerland) supplemented with 2 mM L-glutamine (cat # BE17-605E,
72 Lonza, Basel, Switzerland), 100 U/ml penicillin and 100 µg/mL streptomycin (cat # DE17-602E, Lonza, Basel, Switzerland), and 3% fetal bovine serum (FBS; cat # FBS-12A, Capricorn
74 Scientific, Ebsdorfergrund, Germany).

For the cytotoxicity and plaque assays, the antiviral activity of stenoparib on SARS-CoV-2
76 was assessed *in vitro* using Vero E6 *Cercopithecus aethiops* kidney cells (cat # CRL-1586, ATCC, Manassas, VA, USA) maintained in Eagle's Minimum Essential Medium (EMEM; cat #
78 30-2003, ATCC, Manassas, VA, USA) supplemented with 2% or 10% FBS, 100 U/mL penicillin and 100 µg/mL streptomycin (cat # P0781, Sigma Aldrich, St. Louis, MO, USA), 0.01 M
80 HEPES solution (cat # H0887, Sigma Aldrich, St. Louis, MO, USA), 1 mM sodium pyruvate

(cat # 11360070, ThermoFisher Scientific, Waltham, MA, USA), 1x non-essential amino acids
82 solution (cat # SH3023801, Fisher Scientific, Waltham, MA, USA).

84 ViroSpot reduction assay

The activities of stenoparib and remdesivir were assessed against a *wt* SARS-CoV-2
86 strain (BavPat1/2020), and four additional SARS-CoV-2 variants of concern; *alpha* (B.1.1.7), *beta* (B.1.351) *delta* (B.1.617.2), and *gamma* (P1), hereafter referred to using Greek
88 nomenclature (Table 1). We performed ten, serial 2-fold dilutions of compound, mixed with 100 plaque-forming units (pfu) of virus, and added the mixture to 80% confluent Vero E6 cells
90 growing in multi-well plates. The Vero E6 cells were fixed and stained 20 hours (h) after infection and immunostained with a SARS-CoV/SARS-CoV-2 Nucleocapsid monoclonal
92 antibody (Sino Biological, Wayne, PA, USA) followed by a horseradish peroxidase (HRP)-labeled Goat anti-Mouse IgG (cat # G-21040, Thermo Fisher, Waltham, MA, USA) and
94 TrueBlue Peroxidase Substrate (cat # 5510-0030, Seracare, Milford, MA, USA). Spots were counted using a CTL ImmunoSpot Image Analyzer (Cleveland, OH, USA) as previously
96 described [10]. The EC_{50} values were approximated using package 'drc 3.0-1' in R version 4.1.1 [11, 12]. Percent inhibition was normalized by taking the average fraction of the wells that
98 showed positive staining compared to the control wells with the highest positive staining [10].

100 **Table 1. SARS-CoV-2 variants used in ViroSpot reduction and plaque assays to evaluate antiviral properties of stenoparib and remdesivir.** The *wt*, *alpha*, *beta*, *delta*, and *gamma*
102 strains were used in the ViroSpot reduction assay. The *alpha* strain was used in the plaque assays. The *delta* strain carries an ORF7a deletion which may have the potential to impact

104 virulence [14]. SARS-CoV-2 strain deposition and contribution credits are provided in the Acknowledgements as requested by BEI Resources.

Variant	Pango lineage	Strain	Isolate	Source
wt	-	BavPat1/2020	Germany	European Virus Archive – GLOBAL; 026V-03883
alpha	B.1.1.7	hCoV-19/USA/CA_CDC_5574/2020	California, USA	BEI Resources; NR-54011
beta	B.1.351	hCoV-19/USA/MD-HP01542/2021	Maryland, USA	BEI Resources; NR-55282
delta	B.1.617.2	hCoV-19/USA/PHC658/2021	Tennessee, USA	BEI Resources; NR-55611*
gamma	P.1	Isolate hCoV-19/Japan/TY7-503/2021	Japan	BEI Resources; NR-54982

106

108 # Plaque assay

Vero E6 cells were infected with the SARS-CoV-2 *alpha* variant using a multiplicity of

110 infection (MOI) of 0.1, and the activity of stenoparib was assessed with and without remdesivir using a plaque reduction assay. Following viral infection and treatment with stenoparib and/or

112 remdesivir, cells were overlaid with low melting point agarose (cat # 1613112, BioRad, Hercules, CA, USA), fixed at 120 h post infection with 4.0% paraformaldehyde (cat #

114 AAJ19943K2, Fisher Scientific, Waltham, MA, USA), stained with crystal violet (cat # V5265, Sigma Aldrich, St. Louis, MO, USA), and plaques were manually counted.

116

Cytotoxicity Assay

118 Cytotoxicity was measured using the Promega CytoTox 96 Nonradioactive Cytotoxicity Assay kit (cat # G1780, Promega, Madison, WI, USA) in 50 µL reactions and 96-well format

120 (cat # 161093, Thermo Scientific, Waltham, MA, USA) according to the manufacturer's

protocol. The assay was measured using a BioTeK Synergy HT plate reader (model # 7091000,
122 BioTek, Winooski, VT, USA) set at 490 nm wavelength. Vero E6 cells were assessed for cytotoxicity at 5 days post-infection. Percent cytotoxicity was calculated by dividing the
124 experimental LDH release at 490 nm wavelength (OD_{490}) by the maximum LDH release control and multiplying by 100.

126

Results

128 We explored the activity of stenoparib against a *wt* SARS-CoV-2 strain and four variant strains *alpha*, *beta*, *delta*, and *gamma* (Table 1). Inhibition of virus replication by stenoparib was
130 dose-dependent, with 50% effective concentration (EC_{50}) estimates ranging from 4.1 μM to 24.1 μM across the five virus strains tested (Fig. 1A). Interestingly, the EC_{50} estimate for stenoparib
132 and the *beta* variant (24.1 μM) was 2.8- to 5.8-fold higher than for the *wt*, *alpha*, and *delta* variants, which were 4.1 μM, ($p = 1.19\times10^{-4}$); 8.5 μM, ($p = 7.96\times10^{-9}$); and 8.2 μM, ($p = 0.06$;
134 S1 and S2 Tables). Similarly, the EC_{50} estimate for stenoparib against the *gamma* variant (13.6 μM) was lower than for the *beta* variant (24.1 μM), however this difference was not statistically
136 significant ($p = 0.22$; S1 and S2 Tables). An analogous phenomenon was noted for remdesivir. The *beta* EC_{50} estimate (9.9 μM) was 2.1- to 4.3-fold higher than for the *wt*, *alpha*, *delta*, and
138 *gamma* variants; 3.8 μM, ($p = 2.76\times10^{-5}$); 4.7 μM, ($p = 2.05\times10^{-11}$); 2.3 μM, ($p = 4.97\times10^{-3}$); and 4.1 μM ($p = 2.32\times10^{-4}$), respectively (S1 and S2 Tables). The ViroSpot experiment was
140 conducted using technical quadruplicates per compound concentration, and infected and untreated cells were used as controls.

142

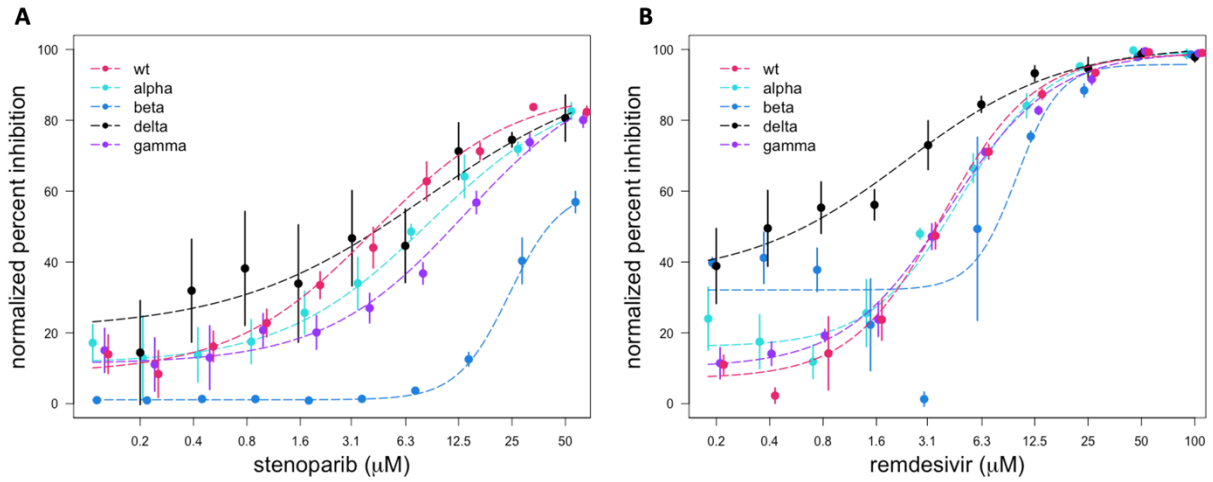

Fig 1. **Dose-response curves for stenoparib and remdesivir on wild type SARS-CoV-2 and four variant SARS-CoV-2 strains.** Normalized percent inhibition (Y-axis) of *wt* SARS-CoV-2 and variant strains *alpha*, *beta*, *delta*, and *gamma* in Vero E6 cells treated with (A) stenoparib and (B) remdesivir at the indicated concentrations (X-axis). Error bars are the standard deviation.

In an additional set of experiments, we focused on the SARS-CoV-2 *alpha* variant. Vero E6 cells were infected with the *alpha* variant using a multiplicity of infection of 0.1, and the activity of stenoparib was assessed with and without remdesivir using the plaque reduction assay. Plaques are areas of dead or destroyed cells and appear as small, clear regions in an infected cell monolayer after fixation and staining with crystal violet. We combined 2.5, 5.0, and 10 μM doses of stenoparib with the previously reported EC_{50} of remdesivir (0.5 μM) [6]. The three control types were 1) infected and untreated cells, 2) uninfected and untreated cells, and 3) infected cells treated with a combination of camostat mesylate and aloxistatin (E64d) (combination hereafter referred to as Camostat-E64d, or 'CE'), which are protease inhibitors that prevent Spike (S) protein cleavage and virus entry into the cell [12].

As shown in Fig. 2A and 2B, neither 10 μM stenoparib nor 0.5 μM remdesivir achieved greater than a 50% reduction in plaquing efficiency compared to the infected, untreated cells.

160 When combined, however, plaque formation was reduced by over 80% compared to infected, untreated cells. This reduction was superior to what was achievable with stenoparib

162 ($p = 3.03\times10^{-5}$) or remdesivir ($p = 1.99\times10^{-4}$) alone at these doses. Notably, cytotoxicity remained near baseline levels (Fig. 2C). The cytotoxicity experiment was run in quadruplicate

164 and cells were treated with CE, dimethylsulfoxide (DMSO), lysis buffer, or left untreated (no compound) as controls. When combined, the activity of two or more drugs with different

166 mechanisms of activity may synergize, with the potential benefit of reducing individual doses of each drug and minimizing undesirable side effects in the patient.

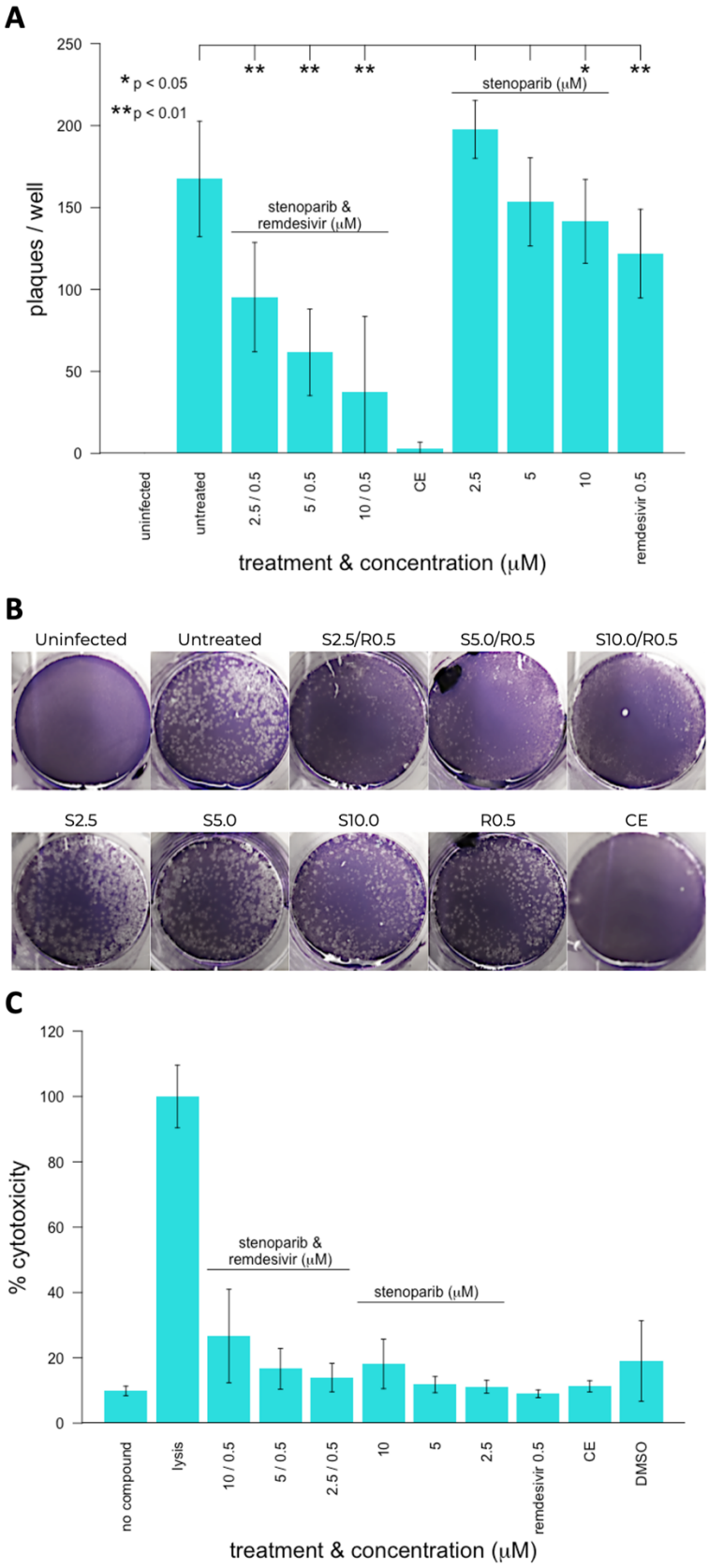
A
250
200
150
100
50
0
plaques / well
* p < 0.05
** p < 0.01
**
**
**
*
**
stenoparib (μM)
stenoparib &
remdesivir (μM)
uninfected
untreated
2.5 / 0.5
5 / 0.5
10 / 0.5
CE
2.5
5
10
remdesivir 0.5
treatment & concentration (μM)
B
Uninfected
Untreated
S2.5/R0.5
S5.0/R0.5
S10.0/R0.5
S2.5
S5.0
S10.0
R0.5
CE
C
120
100
80
60
40
20
0
% cytotoxicity
stenoparib &
remdesivir (μM)
stenoparib (μM)
no compound
lysis
10 / 0.5
5 / 0.5
2.5 / 0.5
10
5
2.5
remdesivir 0.5
CE
DMSO
treatment & concentration (μM)

168

Fig 2. Activity of stenoparib and remdesivir on the *alpha* SARS-CoV-2 variant and
170 **cytotoxicity of stenoparib and remdesivir in Vero E6 cells.** (A) Virus plaque assays. Vero E6 cells were infected for 2 hours with SARS-CoV-2 *alpha* variant, washed, and overlaid with low-
172 melting temp agarose/MEM with or without stenoparib and/or remdesivir at the concentrations indicated. The cell monolayers were fixed with 4% paraformaldehyde and stained with 0.1%
174 crystal violet prior to manual counting of plaques. The experiment was performed using technical triplicates and error bars represent the standard deviation of three independent
176 experiments. For pairwise comparisons to untreated cells, * indicates p-values less than 0.05 and ** indicates p-values less than 0.01. (B) Photographs of plate wells after crystal violet staining.
178 Labels indicate the concentrations of stenoparib or remdesivir. Abbreviations: S = stenoparib, R = remdesivir at the concentrations indicated (i.e. 2.5 / 0.5 = 2.5 μM stenoparib,
180 0.5 μM remdesivir). (C) Cytotoxicity measurements performed by the lactate dehydrogenase release assay (Promega Cytotox 96) 48 hours after infection. Inhibitors stenoparib or remdesivir
182 were used at the indicated concentrations (X-axis). The assays were performed according to the manufacturer's recommendations. Results from drug treatments were normalized to the fraction
184 of maximum cytotoxicity (% Cytotoxicity; Y-axis) achieved by detergent lysis of cells. The samples were processed in triplicate and error bars represent the standard deviation of three
186 independent experiments.

188 # Discussion

According to a recent report, the *beta* variant appears to exhibit a significantly reduced
190 eclipse period (length of time between initial infection and the production of virus by a cell) and more rapid replication *in vitro* compared to the *alpha* variant [14], which could explain the

192 relatively higher stenoparib and remdesivir EC_{50} estimates for the *beta* variant. In addition to numerous changes to the S protein, the *beta* variant carries some unique mutations in the N
194 protein and in the Nsp3 polyprotein (ORF1a) that are not found in the other variants [15], and may be involved in viral degradation pathways including ADPR following infection [16].
196 Differential susceptibility to ADPR may be related to the altered replication kinetics of the *beta* variant, although this awaits further investigation.

198 Besides the known roles for the PARP1 and PARP2 enzymes in DNA repair [17, 18], members of the PARP family have numerous additional functions [19]. The 18 known human
200 PARPs appear to differentially affect viral replication; some exhibit proviral activity and others exhibit antiviral roles [7, 20-24]. In coronavirus, the N protein is mono (ADP) ribosylated
202 (MARylated) during infection. Stability of the N protein is critical for viral genome replication, translation, packaging, and modulation of the host cell cycle [25]. The N protein is the only
204 ADPR target definitively identified in coronavirus thus far [20], and the prevalence of this modification across multiple coronavirus families suggests an important role in virus stability
206 [20]. Despite this, the role of N protein MARylation, and of ADPR in general with regards to coronavirus stability, is not well characterized. Possibly ADPR has a role in regulating virus
208 genome structure, like ADPR of histones or the adenovirus core proteins [26, 27]. While remdesivir and molnupiravir inhibit viral RNA replication, stenoparib likely acts through
210 multiple targets. A combination of stenoparib and remdesivir or molnupiravir may be highly potent at inhibiting SARS-family coronaviruses including SARS-CoV-2.

212 A host-targeting therapeutic like stenoparib could be a significant benefit for COVID-19 patients as a standalone therapy, or especially as part of a combinatorial COVID-19 treatment
214 strategy with an antiviral drug such as remdesivir or molnupiravir. Combinations of two or more

drugs may lead to synergism through different mechanisms of action, which has the potential

216 benefit of reducing individual doses of each drug and minimizing undesirable side effects.

Author contributions

Conceptualization: Christopher T French, Erik W Settles, Steen Knudsen, Paul S Keim

Data curation: Katherine E Zarn

Formal analysis: Katherine E Zarn, Christopher T French, Sierra A Jaramillo

Funding acquisition: Steen Knudsen, Christopher T French, Paul S Keim

Investigation: Katherine E Zarn, Sierra A Jaramillo, Anthony R Zapata, Ashley N Jones, Haley E Nunnally, Aloys SL Tijsma, Patricia M Nuijten

Methodology: Christopher T French, Nathan E Stone

Project Administration: Christopher T French, Paul S Keim, Steen Knudsen, Aloys SL Tijsma

Resources: Christopher T French, Paul S Keim

Supervision: Christopher T French, Erik W Settles, Paul S Keim

Visualization: Ken Ng, Katherine E Zarn

Writing – Original Draft: Christopher T French

Writing – Review & Editing: Katherine E Zarn, Christopher T French, Nathan E Stone, Aloys SL Tijsma

Acknowledgements

The following reagents were obtained through BEI Resources, NIAID, NIH: SARS-Related Coronavirus 2, Isolate USA/CA_CDC_5574/2020, NR-54011, deposited by the Centers for Disease Control and Prevention; SARS-Related Coronavirus 2, Isolate hCoV-19/USA/MD-HP01542/2021 (Lineage B.1.351), in Homo sapiens Lung Adenocarcinoma (Calu-3) Cells, NR-55282, contributed by Andrew S. Pekosz; SARS-Related Coronavirus 2, Isolate hCoV-

19/USA/PHC658/2021 (Lineage B.1.617.2; *Delta* Variant), NR-55611, contributed by Dr. Richard Webby and Dr. Anami Patel; and SARS-Related Coronavirus 2, Isolate hCoV-19/Japan/TY7-503/2021 (Brazil P.1), NR-54982, contributed by National Institute of Infectious Diseases.

Competing interests

SK is employed by and holds a financial interest in Allarity Therapeutics, which stands to potentially benefit from these results.

Funding

This research was supported by a grant from The Flinn Foundation, the Cowden Endowment for Microbiology, and an Arizona Board of Regents TRIF award. Core experiments were supported by service fees paid by Allarity Therapeutics.

References

1. WHO. 2021. Available from: https://covid19.who.int/. Accessed 8 March 2022.
2. Prevention USCfDCa. Information for Clinicians on Investigational Therapeutics for Patients with COVID-19 Centers for Disease Control and Prevention: National Center for Immunization and Respiratory Diseases (NCIRD), Division of Viral Diseases; 2020. Available from: https://www.cdc.gov/coronavirus/2019-ncov/hcp/therapeutic-options.html.
3. Beigel JH, Tomashek KM, Dodd LE, Mehta AK, Zingman BS, Kalil AC, et al. Remdesivir for the Treatment of Covid-19 - Final Report. The New England journal of medicine. 2020;383(19):1813-26. Epub 2020/05/24. doi: 10.1056/NEJMoa2007764. PubMed PMID: 32445440; PubMed Central PMCID: PMCPMC7262788.
4. Kokic G, Hillen HS, Tegunov D, Dienemann C, Seitz F, Schmitzova J, et al. Mechanism of SARS-CoV-2 polymerase stalling by remdesivir. Nat Commun. 2021;12(1):279. Epub 2021/01/14. doi: 10.1038/s41467-020-20542-0. PubMed PMID: 33436624; PubMed Central PMCID: PMCPMC7804290.
5. Kabinger F, Stiller C, Schmitzova J, Dienemann C, Kokic G, Hillen HS, et al. Mechanism of molnupiravir-induced SARS-CoV-2 mutagenesis. Nat Struct Mol Biol. 2021;28(9):740-6. Epub 2021/08/13. doi: 10.1038/s41594-021-00651-0. PubMed PMID: 34381216; PubMed Central PMCID: PMCPMC8437801.
6. Stone NE, Jaramillo SA, Jones AN, Vazquez AJ, Martz M, Versluis LM, et al. Stenoparib, an Inhibitor of Cellular Poly(ADP-Ribose) Polymerase, Blocks Replication of the SARS-CoV-2 and HCoV-NL63 Human Coronaviruses *In Vitro*. mBio. 2021;12(1):e03495-20. doi: 10.1128/mBio.03495-20.
7. Kuny CV, Sullivan CS. Virus-Host Interactions and the ARTD/PARP Family of Enzymes. PLoS pathogens. 2016;12(3):e1005453. Epub 2016/03/25. doi: 10.1371/journal.ppat.1005453. PubMed PMID: 27010460; PubMed Central PMCID: PMCPMC4806868.
8. McGonigle S, Chen Z, Wu J, Chang P, Kolber-Simonds D, Ackermann K, et al. E7449: A dual inhibitor of PARP1/2 and tankyrase1/2 inhibits growth of DNA repair deficient tumors and antagonizes Wnt signaling. Oncotarget. 2015;6(38):41307-23. Epub 2015/10/30. doi: 10.18632/oncotarget.5846. PubMed PMID: 26513298; PubMed Central PMCID: PMCPMC4747407.
9. Thorsell AG, Ekblad T, Karlberg T, Low M, Pinto AF, Tresaugues L, et al. Structural Basis for Potency and Promiscuity in Poly(ADP-ribose) Polymerase (PARP) and Tankyrase Inhibitors. J Med Chem. 2017;60(4):1262-71. Epub 2016/12/22. doi: 10.1021/acs.jmedchem.6b00990. PubMed PMID: 28001384; PubMed Central PMCID: PMCPMC5934274.
10. van Baalen CA, Jeeninga RE, Penders GH, van Gent B, van Beek R, Koopmans MP, et al. ViroSpot microneutralization assay for antigenic characterization of human influenza viruses. Vaccine. 2017;35(1):46-52. Epub 2016/12/03. doi: 10.1016/j.vaccine.2016.11.060. PubMed PMID: 27899226.
11. Ritz C SJ. Package ‘drc’. Analysis of dose-response data is made available through a suite of flexible and versatile model fitting and after- fitting functions. ed. https://cran.r-project.org/web/packages/drc/drc.pdf: CRAN; 2016.

12. Ritz C, Baty F, Streibig JC, Gerhard D. Dose-Response Analysis Using R. PloS one. 2015;10(12):e0146021. Epub 20151230. doi: 10.1371/journal.pone.0146021. PubMed PMID: 26717316; PubMed Central PMCID: PMCPMC4696819.
13. Hoffmann M, Kleine-Weber H, Schroeder S, Kruger N, Herrler T, Erichsen S, et al. SARS-CoV-2 Cell Entry Depends on ACE2 and TMPRSS2 and Is Blocked by a Clinically Proven Protease Inhibitor. Cell. 2020;181(2):271-80 e8. Epub 2020/03/07. doi: 10.1016/j.cell.2020.02.052. PubMed PMID: 32142651; PubMed Central PMCID: PMCPMC7102627.
14. Pyke AT, Nair N, van den Hurk AF, Burtonclay P, Nguyen S, Barcelon J, et al. Replication Kinetics of B.1.351 and B.1.1.7 SARS-CoV-2 Variants of Concern Including Assessment of a B.1.1.7 Mutant Carrying a Defective ORF7a Gene. Viruses. 2021;13(6). Epub 2021/07/03. doi: 10.3390/v13061087. PubMed PMID: 34200386; PubMed Central PMCID: PMCPMC8227137.
15. Hodcroft EB. CoVariants: SARS-CoV-2 Mutations and Variants of Interest 2021. Available from: https://covariants.org/.
16. Lei J, Kusov Y, Hilgenfeld R. Nsp3 of coronaviruses: Structures and functions of a large multi-domain protein. Antiviral Res. 2018;149:58-74. Epub 2017/11/13. doi: 10.1016/j.antiviral.2017.11.001. PubMed PMID: 29128390; PubMed Central PMCID: PMCPMC7113668.
17. Dziadkowiec KN, Gasiorowska E, Nowak-Markwitz E, Jankowska A. PARP inhibitors: review of mechanisms of action and BRCA1/2 mutation targeting. Prz Menopauzalny. 2016;15(4):215-9. doi: 10.5114/pm.2016.65667. PubMed PMID: 28250726; PubMed Central PMCID: PMCPMC5327624.
18. Ame JC, Rolli V, Schreiber V, Niedergang C, Apiou F, Decker P, et al. PARP-2, A novel mammalian DNA damage-dependent poly(ADP-ribose) polymerase. The Journal of biological chemistry. 1999;274(25):17860-8. Epub 1999/06/11. doi: 10.1074/jbc.274.25.17860. PubMed PMID: 10364231.
19. Gupte R, Liu Z, Kraus WL. PARPs and ADP-ribosylation: recent advances linking molecular functions to biological outcomes. Genes & development. 2017;31(2):101-26. doi: 10.1101/gad.291518.116. PubMed PMID: 28202539.
20. Grunewald ME, Fehr AR, Athmer J, Perlman S. The coronavirus nucleocapsid protein is ADP-ribosylated. Virology. 2018;517:62-8. Epub 2017/12/05. doi: 10.1016/j.virol.2017.11.020. PubMed PMID: 29199039; PubMed Central PMCID: PMCPMC5871557.
21. Grunewald ME, Chen Y, Kuny C, Maejima T, Lease R, Ferraris D, et al. The coronavirus macrodomain is required to prevent PARP-mediated inhibition of virus replication and enhancement of IFN expression. PLoS pathogens. 2019;15(5):e1007756. Epub 2019/05/17. doi: 10.1371/journal.ppat.1007756. PubMed PMID: 31095648; PubMed Central PMCID: PMCPMC6521996.
22. Li L, Zhao H, Liu P, Li C, Quanquin N, Ji X, et al. PARP12 suppresses Zika virus infection through PARP-dependent degradation of NS1 and NS3 viral proteins. Science signaling. 2018;11(535):eaas9332. doi: 10.1126/scisignal.aas9332. PubMed PMID: 29921658.
23. Atasheva S, Frolova EI, Frolov I. Interferon-stimulated poly(ADP-Ribose) polymerases are potent inhibitors of cellular translation and virus replication. Journal of virology.

2014;88(4):2116-30. Epub 2013/12/11. doi: 10.1128/JVI.03443-13. PubMed PMID: 24335297.

24. Westera L, Jennings AM, Maamary J, Schwemmle M, Garcia-Sastre A, Bortz E. Poly-ADP Ribosyl Polymerase 1 (PARP1) Regulates Influenza A Virus Polymerase. Adv Virol. 2019;2019:8512363. Epub 2019/04/25. doi: 10.1155/2019/8512363. PubMed PMID: 31015836; PubMed Central PMCID: PMCPMC6444269.

25. McBride R, van Zyl M, Fielding BC. The coronavirus nucleocapsid is a multifunctional protein. Viruses. 2014;6(8):2991-3018. Epub 2014/08/12. doi: 10.3390/v6082991. PubMed PMID: 25105276; PubMed Central PMCID: PMCPMC4147684.

26. Déry CV, de Murcia G, Lamarre D, Morin N, Poirier GG, Weber J. Possible role of ADP-ribosylation of adenovirus core proteins in virus infection. Virus Research. 1986;4(4):313-29. doi: https://doi.org/10.1016/0168-1702(86)90078-X.

27. Strickfaden H, McDonald D, Kruhlak MJ, Haince J-F, Th'ng JPH, Rouleau M, et al. Poly(ADP-ribosyl)ation-dependent Transient Chromatin Decondensation and Histone Displacement following Laser Microirradiation. Journal of Biological Chemistry. 2016;291(4):1789-802. doi: https://doi.org/10.1074/jbc.M115.694992.